The following publication A. Gueye, I. Kocar, E. Francois and J. Mahseredjian, "Comparison of Rational Krylov and Vector Fitting in Transient Simulation of Transmission Lines and Cables," in IEEE Transactions on Power Delivery, vol. 38, no. 5, pp. 3333-3341, Oct. 2023 is available at https://dx.doi.org/10.1109/TPWRD.2023.3272927.

Comparison of Rational Krylov and Vector Fitting in Transient Simulation of Transmission Lines and Cables

Aziz Gueye, *Student Member, IEEE,* Ilhan Kocar, *Senior Member, IEEE,* Emmanuel Francois, *Student Member, IEEE,* and Jean Mahseredjian, *Fellow Member, IEEE*

***Abstract*--This paper presents stringent comparisons between Vector Fitting (VFIT), Relaxed Vector Fitting (R-VFIT) and Rational Krylov Fitting (RKFIT) techniques in the fitting of transmission line and cable functions to rational forms while accounting for the frequency dependence of electrical parameters. The fitting procedures encapsulate new solution strategies to improve fitting performance. Various case studies are presented to assess the performance of RKFIT in terms of model order reduction, passivity violation and computing times. In addition, the use of RKFIT in obtaining the frequency dependent cable model (FDCM) is demonstrated for the first time together with a resolved case study that showed unstable behavior with the universal line model (ULM) methodology.**

***Index Terms*-- Electromagnetic transients, line constants, cable constants, rational Krylov approximation, Universal Line Model (ULM), Frequency Dependent Cable Model (FDCM)**

I. Introduction

THE distributed parameter models and transient analysis of transmission lines and cables in electromagnetic transient (EMT) programs are based on traveling wave equations and the use of two frequency dependent functions: the characteristic admittance matrix $\mathbf{Y_c}$ and the propagation matrix $\mathbf{H}$. The basic idea of EMT models is to use rational function approximations for these functions obtained by different fitting techniques. The rational functions are used in EMT simulations for fast and efficient computations of convolution integrals in the time domain through recursive schemes to reproduce frequency dependent behavior.

The Universal Line Model (ULM) [1] based on Vector Fitting (VFIT) technique [2] or its successor with improved pole relocation, Relaxed Vector Fitting (R-VFIT) [3], is widely adopted in EMT-type programs. The VFIT solves a least squares (LS) problem on a projection space represented in the partial fraction basis. It delivers high model precision and computational accuracy. In the ULM, there are three main steps in the fitting of $\mathbf{H}$. First, the matrix is transformed into modal domain at each frequency sample. Second, each modal propagation function, i.e., mode or eigenvalue of $\mathbf{H}$ is fitted to a rational function multiplied by an exponential delay term. Then, using the poles and delays, the residues of $\mathbf{H}$ are solved using LS technique. This approach may lead to numerically unstable models for cables with many conductors due to unbalanced fitting in phase domain, and amplified interpolation and integration errors. One solution to alleviate these errors is to use more precise interpolation and integration techniques [4]. Another solution is to use the frequency dependent cable model (FDCM) of [5]. In this model, similar or repetitive eigenvalues are grouped and their grouped contributions in phase domain are fitted with a single delay term with the objective of avoiding high residue-pole ratios with opposite signs from different modal groups. The individual contributions of eigenvalues or modal contributions are called idempotents. Fitting idempotents of repetitive or coalescing eigenvalues would be complex due to their non smooth characteristics. This was overlooked in early idempotent models [6], [7].

A new approach based on partitioned fitting and DC correction is proposed in [8] and can be used together with different models where higher accuracy near DC frequencies is required. This approach is complementary to existing models but can help solving passivity problems in some cases.

A new rational approximation method based on Rational Arnoldi Decomposition (RAD) has been recently proposed [9], [10], [11], [12]. The new Rational Krylov Fitting (RKFIT) technique is applied by using a projection space characterized with discrete orthogonal rational functions and solves an LS problem as in the VFIT technique. The main difference between RKFIT and VFIT is the process of the relocation of poles. RKFIT is available as a toolbox in MATLAB environment [11].

The ULM based on RKFIT was first introduced in [13], where only two simple illustrative examples of transmission systems with one and three conductors were presented. According to [13], RKFIT typically produces a smaller number of poles in the fitting of modes of $\mathbf{H}$ when compared to R-VFIT.

One of the goals in this paper is to achieve a comprehensive numerical comparison of RKFIT and VFIT through challenging cases for both cable and line systems. The original contribution of this paper is to present the performance of RKFIT using two different models, i.e., FDCM and ULM. The application of

Aziz Gueye, Polytechnique Montreal, Canada (aziz.gueye@polymtl.ca)
Ilhan Kocar, The Hong Kong Polytechnic University, Hong Kong SAR China (ilhan.kocar@polyu.edu.hk)
Emmanuel François, Polytechnique Montréal, Canada (emmanuel.francois@polymtl.ca)
Jean Mahseredjian, Polytechnique Montreal, Canada (jean.mahseredjian@polymtl.ca)

RKFIT in fitting matrix functions with a common set of poles is also presented. This is a must for FDCM to achieve vectorized and fast computations in time domain. In addition, it is shown with case studies that RKFIT is helpful in obtaining stable models but can still encounter passivity violations.

This paper starts by first presenting the RKFIT algorithm and its application to the fitting of line and cable functions in matrix forms and in the phase domain using a common set of poles. The ULM and FDCM methods with improved solution strategies are presented in section III. Numerical comparisons are presented in section IV.

II. Presentation Of The RKFIT Algorithm

Given a frequency dependent characteristic admittance matrix,

$$\mathbf{Y_c}(s)=\begin{bmatrix} y_{11}(s) & \cdots & y_{1N_c}(s) \\ \vdots & \ddots & \vdots \\ y_{N_c1}(s) & \cdots & y_{N_cN_c}(s) \end{bmatrix} \tag{1}$$

where the frequency $s=j\omega$ is in rad/s, and the subscript N_c denotes the number of conductors of the transmission system, the goal is to use the RKFIT algorithm to produce a rational model of $\mathbf{Y}_c$ in the following representation

$$\mathbf{Y_c} \cong \mathbf{C}_0 + \sum_{i=1}^{M} \frac{1}{s-q_i}\mathbf{C}_i \tag{2}$$

where $\mathbf{C_0}$ is a constant matrix corresponding to $\mathbf{Y_c}$ when $s\to\infty$, M is the order of the fit, q_i represents the i^{th} pole and $\mathbf{C}_i$ is the corresponding matrix of residues. The RKFIT algorithm is a fitting method based on rational Krylov space. It iteratively tries to approximate $\mathbf{Y_c}$ in the form of (2) by solving nonlinear rational least square problems. In this paper, we will provide the presentation of RKFIT algorithm applied to $\mathbf{Y_c}$. The same principle applies to the modal decomposition or groups of the propagation matrix $\mathbf{H}$, once the delay component is extracted. General analysis on rational Krylov fitting is presented in [9], [14]-[17].

Given a square matrix $\mathbf{A}$ with a size of $N\times N$ and a starting vector $\mathbf{b}$ with a size of $N\times 1$, let $\Lambda(\mathbf{A})$ be the set of all eigenvalues of $\mathbf{A}$, and q_m a polynomial function

$$q_m(z)=\prod_{j=1,\zeta_j\neq\infty}^{m} z-\zeta_j \tag{3}$$

such that $\zeta_1,\zeta_2,...,\zeta_m \notin \Lambda(\mathbf{A})$. A polynomial Krylov space of order $m+1$ is defined as

$$\mathbb{K}_{m+1}(\mathbf{A},\mathbf{b}) = span\left\{\mathbf{b},\mathbf{Ab},...\mathbf{A}^m\mathbf{b}\right\} \tag{4}$$

The rational Krylov space of order $m+1$ associated with $\mathbf{A}$, $\mathbf{b}$ and ζ_j is defined as

$$\begin{aligned} Q_{m+1}(\mathbf{A},\mathbf{b},q_m) &= q_m(\mathbf{A})^{-1}\,\mathbb{K}_{m+1}(\mathbf{A},\mathbf{b}) \\ &= q_m(\mathbf{A})^{-1}\,span\left\{\mathbf{b},\mathbf{Ab},...\mathbf{A}^m\mathbf{b}\right\} \end{aligned} \tag{5}$$

where $q_m(z)$ is the common denominator of the rational functions associated with the rational Krylov space. Since the roots of the polynomial q_m, $\zeta_1,\zeta_2,...,\zeta_m \notin \Lambda(\mathbf{A})$, $q_m(\mathbf{A})^{-1}$ exist $Q_{m+1}(\mathbf{A},\mathbf{b},q_m)$ is well defined. In order to extract information from (5), an RAD of the space $Q_{m+1}(\mathbf{A},\mathbf{b},q_m)$ that satisfies

$$\mathbf{A}\mathbf{V}_{m+1}\underline{\mathbf{K}_m} = \mathbf{V}_{m+1}\underline{\mathbf{H}_m} \tag{6}$$

is performed, where $\left(\underline{\mathbf{H}_m},\underline{\mathbf{K}_m}\right)$ is an unreduced $(m+1)\times m$ upper Hessenberg pencil and $\mathbf{V}_{m+1}$ an orthonormal basis of the space $Q_{m+1}(\mathbf{A},\mathbf{b},q_m)$. The rational Krylov space of order $m+1+k$, such that $k+m\geq 0$, is defined as $Q_{m+1+k}(\mathbf{A},\mathbf{b},q_m)$. Therefore (6) can be extended or truncated in the following general form

$$\mathbf{A}\mathbf{V}_{m+1+k}\underline{\mathbf{K}_{m+k}} = \mathbf{V}_{m+1+k}\underline{\mathbf{H}_{m+k}} \tag{7}$$

If $k=0$, (6) and (7) coincide. The RKFIT algorithm uses a search $S_{space}=R(\mathbf{V}_{m+1})$ which is simply $Q_{m+1}(\mathbf{A},\mathbf{b},q_m)$ expressed in its orthonormal basis and a target space $T_{space}=R(\mathbf{V}_{m+1+k})=Q_{m+1+k}(\mathbf{A},\mathbf{b},q_m)$ which is an extension of the basis $\mathbf{V}_{m+1}$ by adding $k\geq 0$ poles at infinity to the poles of q_m or a truncation of $\mathbf{V}_{m+1}$ by considering only the first $m+1+k$ column of $\mathbf{V}_{m+1}$ for $k<0$. Both are linear spaces in $\mathbb{C}^N$ used in the pole relocation process. The search space is used to search for poles so that LS approximation is improved in the target space.

We now show how the RKFIT algorithm is applied to the fitting of the characteristic admittance matrix $\mathbf{Y_c}$ and the pole relocation process. The goal here is to provide a comprehensive overview of the RKFIT algorithm applied using the rational Krylov toolbox in MATLAB [11] to perform our computations. Let's consider first the simple case of fitting one single element $y_{11}(s)$ of $\mathbf{Y_c}$. We will generalize this idea to fit all the elements of $\mathbf{Y_c}$ at once using a common set of poles. Given the frequency samples data in a matrix form:

$\mathbf{S}=diag(s_i)\in\mathbb{C}^{N_s\times N_s}$ and $\mathbf{F}=diag(f_i)\in\mathbb{C}^{N_s\times N_s}$ with $f_i=y_{11}(s_i)$, $i=1...N_s$, N_s is the number of frequency samples, stating column vector $\mathbf{b}\in\mathbb{C}^{N_s}$ for constructing the Krylov space, where $b_{i1}=1$ for all $i=1,\ldots N_s$. The algorithm attempts to find a rational function,

$$r=\frac{p_{m+k}}{q_m} \tag{8}$$

where p_{m+k}, and $\left\{\mathbf{w}^j\right\}_{j=1}^{l}$ are polynomials of degree at most $m+k$ and m respectively such that the relative error

$$\varepsilon_{rel}=\frac{\left\|\mathbf{Fb}-r(\mathbf{S})\mathbf{b}\right\|_2}{\left\|\mathbf{Fb}\right\|_2}\to\min, \tag{9}$$

is minimal. At first, a RAD of the search space $Q_{m+1}(\mathbf{S},\mathbf{b},q_m)$ that satisfies (6) is computed. Then the rational approximation (8) is the solution of the minimization in (9). Let $\mathrm{P}_{T_{space}}=\mathbf{V}_{m+1+k}\mathbf{V}^{*}_{m+1+k}$ denote the projection onto the target space $T_{space}=Q_{m+1+k}(\mathbf{S},\mathbf{b},q_m)$. $r(\mathbf{S})\mathbf{b}$ is the orthogonal project of the vector $\mathbf{Fb}$ onto the target space. Hence (9) is equivalent to look for a unit 2-norm vector $\mathbf{v}\in S_{space}$ such that

$$\left\|\mathbf{Fv}-\mathbf{V}_{m+1+k}\mathbf{V}^{*}_{m+1+k}\mathbf{Fv}\right\|_2 \tag{10}$$

is minimal. A solution to this is given by $\mathbf{v}=\mathbf{V}_{m+1}\mathbf{c}$ where $\mathbf{c}$ is the right singular vector of the matrix $(I-P_{space})\mathbf{FV}_{m+1}$ associated with the smallest singular value σ_{m+1}. The pole relocation procedure is now to iteratively find a new polynomial $\hat{q}_m$ that has no roots in the set of eigenvalues of $\mathbf{S}$ such that

$$\mathbf{V}_{m+1}\mathbf{c}=\hat{q}_m(\mathbf{S})q_m(\mathbf{S})^{-1}\mathbf{b}\,. \tag{11}$$

The model order reduction is guaranteed by Theorem 6.1 in [9] if the fitting tolerance ε_{tol} allows it. More specifically, the model order is reduced with the largest integer

$$r\le\min(m,m+k)\quad\text{such that}\quad\sigma_{m+1-r}\le\left\|\mathbf{Fb}\right\|_2\varepsilon_{tol} \tag{12}$$

RKFIT is extended to fit all the elements of $\mathbf{Y_c}$ at once with the same set of poles. Specifically, for a given frequency sample $\mathbf{S}=diag(s_i)\in\mathbb{C}^{N_s\times N_s}$, a family of $l=N_c\times N_c$ matrices $\left\{F^j\right\}_{j=1}^{l}$, where each $F^j=diag\left(f_i{}^j\right)$ and $f_i{}^j$ is the result of the j^{th} element of $\mathbf{Y_c}$ evaluated at s_i for all $j=1,...,l$. The algorithm searches for a set of rational functions

$$\left\{r^j=\frac{p^j_{m+k}}{q_m}\right\}_{j=1}^{l} \tag{13}$$

with all functions having a common denominator q_m while ensuring that the relative error

$$\varepsilon_{rel}=\sqrt{\frac{\sum_{j=1}^{l}\left\|\mathbf{W}^j\left[\mathbf{F}^j\mathbf{b}-r^j(\mathbf{S})\mathbf{b}\right]\right\|^2}{\sum_{j=1}^{l}\left\|\mathbf{W}^j\mathbf{F}^j\mathbf{b}\right\|^2}} \tag{14}$$

is minimal. The family of l matrices $\left\{\mathbf{W}^j\right\}_{j=1}^{l}$ is an optional weighting scheme and if not provided, $\mathbf{W}^j=\mathbf{I}_{N_s}$ for all $j=1,...,l$. Note that (14) contains (9) for $l=1$ and $\mathbf{W}^j=I_{N_s}$. In fact, since all the elements of $\mathbf{Y_c}$ share the same input of frequency samples $\mathbf{S}=diag(s_i)\in\mathbb{C}^{N_s\times N_s}$, we need to use only one Krylov search space $S_{space}=Q_{m+1}(\mathbf{A},\mathbf{b},q_m)$ for the rational approximation of all the family $\left\{F^j\right\}_{j=1}^{l}$. This guaranties all the $\left\{F^j\right\}_{j=1}^{l}$ sharing the same set of poles. The only difference now from the case where $l=1$ is, we need to compute l different projection space $\mathrm{P}^j_{T_{space}}=\mathbf{V}^j_{m+1+k}\mathbf{V}^{j*}_{m+1+k}$, one related to each $\left\{F^j\right\}_{j=1}^{l}$ while minimizing (14). Each element of the characteristic admittance matrix can be then approximated with a rational function r^j by the coefficient vector

$$\mathbf{c}^j=\left(\mathbf{W}^j\mathbf{V}_{m+1+k}\right)^{\dagger}\left(\mathbf{W}^j\mathbf{F}^j\mathbf{b}\right)/\left\|\mathbf{b}\right\|_2 \tag{15}$$

where † denotes the pseudo-inverse (see [9]). This feature allows us to fit all the elements of $\mathbf{Y_c}$ together using a common set of poles. In order to make the fitting results compatible with the Wideband time domain simulation algorithm in EMTP [23], the complete problem of fitting $\mathbf{Y_c}$ is transformed into real form by applying suitable transformations. Therefore, the fitting results come in complex conjugate residues and poles as in the VFIT algorithm. The inputs are: a matrix $\mathbf{S}\in\mathbb{C}^{N_s\times N_s}$ of frequency samples in real form, a set of matrices $\left\{F^j\right\}_{j=1}^{l}\subset\mathbb{C}^{N_s\times N_s}$ representing the elements of $\mathbf{Y_c}$ in real matrix form, a vector $\mathbf{b}\in\mathbb{C}^{N_s}$ and an initial guess $q_m\in P_m$ for the denominator, integer $\left\{\mathbf{W}^j\right\}_{j=1}^{l}\subset N_c\times N_c$ such that k to control the order of the numerator and denominator, $k+m\ge 0$ which is tolerance to apply to model order reduction, flags real and reduction to perform a fitting in real form and apply a model order reduction if the errors allow it, and maxit which is the maximum number of iteration for poles relocation. Optional input of a family of weighting scheme, $\left\{\mathbf{W}^j\right\}_{j=1}^{l}\subset N_s\times N_s$ can be added to the input parameter for speed and if not provided, they are all set to identity. The outputs are: a Rational Arnoldi Decomposition RAD (6) and vectors $\left\{c^j\right\}_{j=1}^{l}$ (15) showing the approximations (13).

The theory above is also used to fit modal contributions in the propagation function matrix $\mathbf{H}$ in phase domain following the extraction of time delays. The propagation function $\mathbf{H}$ is given by $\mathbf{H}=e^{-\mathbf{\Gamma}\mathrm{L}}$ with $\mathbf{\Gamma}=\sqrt{\mathbf{YZ}}$. $\mathbf{Y}$ and $\mathbf{Z}$ are $N_c\times N_c$ coupled matrices per unit length representing frequency dependent shunt admittance and series impedance matrices respectively, and L is the length of the cable.

The complete high-level steps of the RKFIT algorithm applied to a single element or the trace of $\mathbf{Y_c}$ (*ytr*) are summarized in Fig. 1 in a flowchart. The extension to matrix fitting is done by creating a cell structure for each entry of the matrix when populating the **F** matrix.

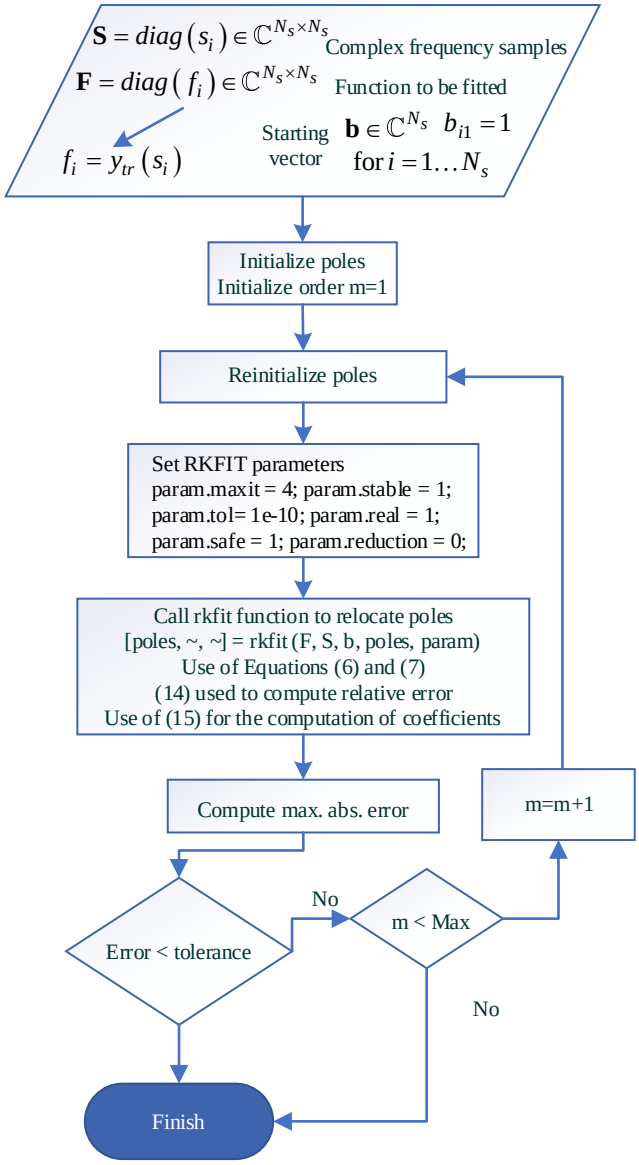

Fig. 1. Flowchart summarizing the application of RKFIT.

III. Presentation Of The Fitting Procedure

In the ULM, the likelihood of high residue-pole pairs from different modal contributions with opposite signs can be reduced to an extent by grouping the delays and modes, but over grouping will make the fitting less accurate. Even though the phases of some modal propagation functions are similar at a given single reference frequency sample used for grouping, their magnitude and phase characteristics for the entire frequency range of interest may be different. This subject is already discussed in the literature, and it is recommended to consider the complex form of modal propagation functions over the entire frequency range of interest to reduce the risk of unbalanced models [4], [18], [19].

Another solution to avoid high residue-pole pairs is the use of the FDCM. In this paper, we present two different modeling approaches generated with the RKFIT algorithm. The first one uses the ULM approach, and the second one uses the FDCM [5], [8] approach where the fitting is performed in the phase domain by directly fitting modal contributions. Although these models are available in the literature, the main structures and implementation details are summarized below to demonstrate how RKFIT is implemented in these models. The improved implementation of the FDCM allows integrating a time delay search algorithm in an efficient manner.

A. ULM Approach

In the ULM, as shown above, all the elements of $\mathbf{Y_c}$ are directly fitted in the phase domain with RKFIT using the same set of poles and $\mathbf{Y_c}$ is expressed in the form of (2). This is different than the original ULM methodology in which the set of poles are identified using the trace of $\mathbf{Y_c}$. VFIT and R-VFIT can also be applied to identify $\mathbf{Y_c}$ directly in the phase domain using a common set of poles. Phase domain and trace fitting methodologies are tested using RKFIT, VFIT, and R-VFIT in the next section.

For the propagation function $\mathbf{H}$, we first compute its modal decomposition:

$$\mathbf{H} = \mathbf{T}\mathbf{H_m}\mathbf{T^{-1}} \tag{16}$$

where $\mathbf{T}$ is the matrix of eigenvectors of the $\mathbf{YZ}$ product and $\mathbf{H_m}$ is a diagonal matrix such as

$$\mathbf{H_m} = diag\left[e^{\lambda_1}, e^{\lambda_2}, \cdots, e^{\lambda_N}\right]$$

with λ_i are the eigenvalues of $-\sqrt{\mathbf{YZ}}\,\mathrm{L}$, e^{λ_i} are the eigenvalues of $\mathbf{H}$, which is also tagged as the modal propagation function H_i or simply mode, and N is the number of conductors. If applicable, grouping is applied based on similarity of eigenvalues. Then, we identify poles and delays of each mode and/or group using RKFIT in the following form:

$$H_i \cong \sum_{k=1}^{M_i} \frac{c_k}{s - p_{i,k}} e^{(-s\tau_i)} \tag{17}$$

where M_i is the number of poles of the rational function for the *i–th* mode/group and $p_{i,k}$ is *k–th* pole of the *i–th* mode/group with c_k being its residue. For the approximation of $\mathbf{H}$ in the phase domain, only the delays and poles of (17) are used. The residues are found using LS technique:

$$\left| \mathbf{H} - \sum_{i=1}^{K} \sum_{k=1}^{M_i} \frac{\mathbf{R}_{i,k}}{s - p_{i,k}} e^{-s\tau_i} \right|_{\min} \tag{18}$$

where K is the number of modes/groups, M_i is order of fitting for each mode/group, τ_i is the time delay, $p_{i,k}$ and $\mathbf{R}_{i,k}$ are the poles and their corresponding residue matrices.

B. FDCM Approach

In the FDCM model, each modal contribution group is fitted with RKFIT to obtain the residues and common set of poles of $\mathbf{H}$ simultaneously. This model is used if the ULM produces numerically unstable models. The key steps in FDCM are summarized below [5], [8].

1) Step 1: Modal decomposition and reconstruction

A modal factorization of the propagation matrix is performed to decompose it into single delay terms. $\mathbf{H}$ is then

expressed as in (16). Let $\mathbf{D}_i$ be a matrix computed by multiplying the *i–th* column of $\mathbf{T}$ by the *i–th* row of $\mathbf{T}^{-1}$. Then (16) can also be written as:

$$\mathbf{H} = \sum_{i=1}^{N} \mathbf{D}_i \, \mathrm{e}^{\lambda_i} \tag{19}$$

It is also possible to decompose (19) by extracting constant delay terms:

$$\mathbf{H} = \sum_{i=1}^{N} \mathbf{D}_i \, e^{\tilde{\lambda}_i} e^{-s\tau_i} = \sum_{i=1}^{N} \tilde{\mathbf{H}}_i e^{-s\tau_i} \tag{20}$$

where $\tilde{\mathbf{H}}_i$ multiplied with the time delay represents the contribution of mode i, and $\tilde{\lambda}_i$ is obtained from λ_i by removing the delay term multiplied by s.

2) Step 2: Computation of delays

In this step, the objective is to compute the constant delay terms using Bode's equations characterizing the relationship between the magnitude and phase of a minimum-phase function [20], [21], [22]. The idea is to compensate the excessive phase lag in propagation modes by removing a delay term while minimizing the order of the fit and fitting error. Note that, similar to electrical parameters, propagation velocities are also frequency dependent so are time delays. Both delays and velocities can be computed by using the complex part of λ_i, i.e., the phase of each propagation mode. Afterwards, each propagation mode can be represented as a minimum phase system accounting for the frequency dependence of its delay multiplied by a constant delay term.

3) Step 3: Grouping

The contribution of a mode is not necessarily a smooth function of frequency. This is explained with eigenvalue perturbation theory and the presence of repetitive or similar eigenvalues. At this stage, similar modes are identified and grouped by adding them. A single delay is assigned to each set of modal contributions. The resulting grouped contributions are smooth functions of frequency. Equation (20) is now given by

$$\mathbf{H} = \sum_{i=1}^{N_r} \hat{\mathbf{H}}_i e^{-s\tau_i} \tag{21}$$

where N_r is the number of groups in the reduced rank of $\mathbf{H}$.

In the new implementation of FDCM, grouped propagation modes are first fitted to identify an initial set of poles together with time delays minimizing the fitting error in the modal domain. The main purpose is to avoid the time delay search process in the fitting of modal contributions in phase domain. Combining time delay optimization together with residue and pole identification in the phase domain at each incremental order can result in heavy run times for systems with several conductors, i.e., systems with around 20 conductors or more.

4) Step 4: Application of RKFIT

After the computations of delays and an initial set of poles, the remaining unknowns in (21) are $\hat{\mathbf{H}}_i$ terms. For each term, the residue matrix and common set of poles are simultaneously calculated using the expression below and by applying RKFIT.

$$\left| \sum_{i=1}^{M_i} \frac{\mathbf{R}_{i,k}}{s - p_{i,k}} - \hat{\mathbf{H}}_i \right|_{\min} \tag{22}$$

Poles coming from the fitting of modes are used as an initial set of guesses to identify poles and residues of modal contributions in the phase domain. If the fitting does not converge, the model order is increased. At this stage, poles are reinitialized using the poles coming from modes and additional poles that are logarithmically spaced.

The error criterion for a modal contribution is set based on the tolerance and maximum absolute value of the contribution. The objective in precising such a criterion is to reach the tolerance in final fitting and well represent the modes with different weighting. On the other hand, increasing the order may result in rank deficiency in some cases and does not reduce the fitting error. In that case, the order with minimum fitting error is retained.

IV. Comparisons Between RKFIT, VFIT, and R-VFIT

In this section, we compare the fitting accuracy and model order in the fitting of the two frequency dependent functions, using the ULM and FDCM approaches. The passivity violation characteristics are also presented for the modeling and fitting approaches used in cable and transmission line systems. Various line and cable configurations are studied. The resulting models are used in time domain simulations. The same time domain solver is used for both ULM and FDCM using the generic phase domain model called the Wideband (WB) model in EMTP [5], [18], [23]. For each case study the resulting fitting errors, model order, and residue-pole ratios that may indicate instability in the time domain are presented. In addition, fitting results with fixed model orders are also presented to show the difference in accuracy between the fitting algorithms from another perspective.

High residue-pole ratios coupled with passivity violations at certain frequency samples typically lead to unstable models. A model is passive if and only if the Hermitian part of the admittance matrix has only positive eigenvalues. The Hermitian part is given as follows:

$$\mathbf{Y}_H(s) = \mathbf{Y}_n(s) + \mathbf{Y}_n^*(s) \tag{23}$$

where $\mathbf{Y}_n^*(s)$ is the conjugate transpose of the transfer admittance matrix $\mathbf{Y}_n(s)$.

The fitting is initialized with logarithmically spaced poles in the frequency range of interest. The model order is increased by one, until convergence or optional stopping criterion, which is twenty poles for $\mathbf{Y_c}$ and H_i in the ULM. In the fitting of H_i, a search algorithm that finetunes time delays is combined with fitting to minimize the fitting error. The search is performed at each order step. The adjustment of time delays is done in small steps, and VFIT is applied for three times for the relocation of poles at each step.

In the ULM, the overall convergence tolerance for $\mathbf{H}$ is based on the maximum difference in absolute values between the input and fitted functions. This is called the maximum absolute error in this paper. The tolerance can be considered as

per unit or percentage since the maximum absolute value of **H** is capped by unity. In case of $\mathbf{Y_C}$, a tolerance based on maximum relative error is used in the existing ULM implementations. This is equal to the maximum absolute error divided by the maximum absolute value of $\mathbf{Y_C}$ at each frequency sample which can be in the order of 0.1. For both functions, two different tolerances are considered, i.e., 0.01 (1%) and 0.001 (0.1%). 1% of tolerance brings very low 2-norm errors for $\mathbf{Y_C}$.

The simulations are performed using a 64 GB RAM computer, Intel Xeon CPU E3 1505M v6 3 GHz equipped with MATLAB 2020a.

1) Case-1: Overhead Transmission Line, 3-phases

This case is for a 3-phase transmission line shown in Fig. 2. Line data is presented in TABLE I . The objective here is to compare the fitting performances using a basic test setup.

The fitting results of **H** are presented in TABLE II and III for different tolerance settings. Max stands for maximum and abs stands for absolute. RKFIT achieves a lower model order for **H** compared to VFIT, however compared to R-VFIT the model order is the same or larger for different tolerance settings.

The fitting results of $\mathbf{Y_C}$ are presented in TABLE IV and TABLE V using the trace and phase fitting methodologies respectively. VFIT results in minimum number of poles for a tolerance on the relative maximum absolute error. Fitting in phase reduces the 2-norm error for a given model order but requires a greater number of poles to achieve the tolerance in relative maximum absolute error. Note that, all the fitting algorithms identify the unknowns using a 2-norm formulation in the end even though the formulations are stated in different way. The reason that the stopping criterion is on the maximum absolute error in ULM is to ensure a precise fitting over all the samples.

For a fixed model order, although all the 2-norm errors are very small, it is observed that R-VFIT produces the least with trace fitting and the global least with phase domain fitting.

For the rest of the cases, phase domain fitting approach will be considered in the fitting of $\mathbf{Y_C}$, and the focus will be on the comparison of R-VFIT with RKFIT in the fitting of **H** given their superior performance.

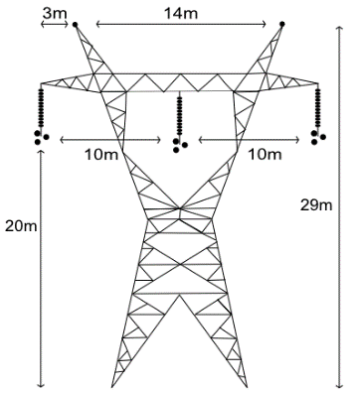

Fig. 2. Case-1, 230 kV three-phase transmission line system, 193.1 km

TABLE I CASE-1, CONDUCTORS DATA

Ground wire radius	4.75 mm
Ground wire DC resistance	3.75 Ohm/km
Bundle radius	230.09 mm
Angle (deg)	0°
Conductor radius	15.29 mm
Conductor DC resistance	0.0701 Ohm/km

TABLE II CASE-1, FITTING RESULTS, **H**

ULM	VFIT	R-VFIT	RKFIT
Tolerance	1%	1%	1%
H model order	25	16	16
H max abs error	0.0024	0.0040	0.0030
Max res/pole ratio	0.78	0.54	0.45
Passivity violation	No	No	No

TABLE III CASE-1, FITTING RESULTS, **H**, REDUCED TOLERANCE

ULM	VFIT	R-VFIT	RKFIT
Tolerance	0.1%	0.1%	0.1%
H model order	30	23	26
H max abs error	4.9x10e-4	8.06 x10e-4	5.82 x10e-4
Max res/pole ratio	3.06	0.78	0.86
Passivity violation	No	No	No

TABLE IV CASE-1, TRACE METHOD, FITTING RESULTS $\mathbf{Y_C}$

ULM	VFIT	R-VFIT	RKFIT
Tolerance	1 %	1 %	1 %
Model order	9	10	13
Relative max abs error	0.0092	0.0063	0.0077
2-norm error	1.27e-06	1.02e-06	2.61e-07
Fixed Order	10	10	10
2-norm error	7.02e-07	6.43e-07	8.34e-07

TABLE V CASE-1, PHASE METHOD, FITTING RESULTS $\mathbf{Y_C}$

ULM	VFIT	R-VFIT	RKFIT
Tolerance	1 %	1 %	1 %
Model order	13	14	15
Relative max abs error	0.0067	0.010	0.0062
2-norm error	$1.46\text{x}10^{-7}$	$1.12\text{x}10^{-7}$	$6.96\text{x}10^{-8}$
Fixed Order	10	10	10
2-norm error	4.25e-07	3.87e-07	5.61e-07

2) Case-2: Short Overhead Transmission Line, 3-phases

This test case is a 5-conductor transmission line system as shown in Fig. 3. Line data is presented in TABLE VI . This case is more complex than Case-1 due to the increased number of conductors and the short line length (420 m). The fitting results are presented in TABLE VII . It is observed that, the ULM models produced by RKFIT, R-VFIT, and VFIT have similar fitting precisions. However, RKFIT and R-VFIT produce a smaller and identical model order in the fitting of **H**.

Fig. 4 shows the voltage waveforms on phase-a. The line is energized with a 230 kV voltage source. The switch closing times are: 0 s on phase-a, 6.4 ms on phase-b, and 4 ms on phase-c. The simulation time-step is $0.1\mu s$. R-VFIT and RKFIT generated models overlap whereas VFIT generated model shows slightly less damping.

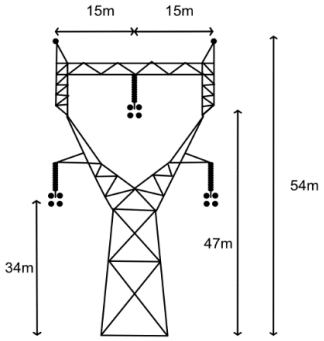

Fig. 3. Case-2, 230 kV overhead-line, 420 m

TABLE VI CASE-2, CONDUCTOR DATA

Ground wire radius	9.6 mm
Ground wire DC resistance	3.330 Ohm/km
Bundle radius	200 mm
Angle (deg)	0°
Conductor radius	15.525 mm
Conductor DC resistance	0.0583 Ohm/km

TABLE VII CASE-2, FITTING RESULTS

ULM	VFIT	R-VFIT	RKFIT
Tolerance	1%	1%	1%
H model order	14	7	7
Tolerance	0.1%	0.1%	0.1%
H model order	16	14	12
Passivity violation	No	No	No

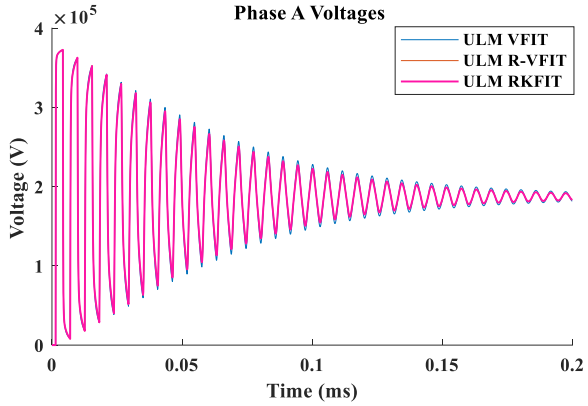

Fig. 4. Case-2, voltages at line end, VFIT, R-VFIT and RKFIT with ULM

3) Case-3: Underground Cable, 3-Phases

The cable system is shown in Fig. 5. Case data is given in Fig. 6 and TABLE VIII . The fitting results are presented in TABLE IX . RKFIT and R-VFIT have similar precisions in line with the fitting tolerance whereas RKFIT achieves a slightly lower model order for the lower tolerance setting. No passivity violation is observed.

In general, the FDCM complements the ULM in case of unstable models, which is not the case here, but for the sake of performing comparisons, the FDCM is also tested. The results show that the application of RKFIT does not reduce the modeling order in FDCM.

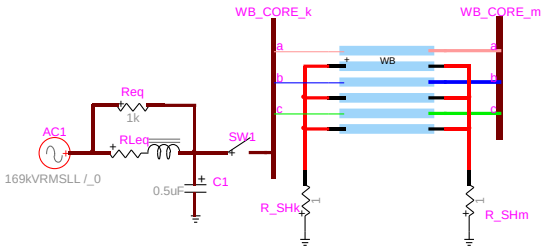

Fig. 5. Case-3, cable system, 3 cables, study system

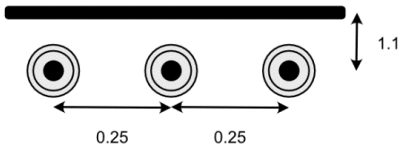

Fig. 6. Case-3, cable system, 3 cables, layout

TABLE VIII CASE-3, CABLE PARAMETERS

Length	15 km
Inner radius of the core	3.18 mm
Outer radius of the core	12.54 mm
Inner radius of the sheath	22.74 mm
Outer radius of the sheath	26.23 mm
Outer insulation radius	29.34 mm
Resistivity of the sheath	2.1×10^{-7} Ohm m
Resistivity of the core	1.7×10^{-8} Ohm m
Core insulator relative permittivity	3.5
Shield insulator relative permittivity	2
Insulation loss factor	4×10^{-4}
Earth resistivity	100 Ohm m

Note that, since increasing the order does not result in high ratio residue-pole pairs with reverse signs in FDCM, a high order model can be used to increase the precision. Also, the fitting is done per modal contribution, and it is not straightforward to control the overall tolerance in multi conductor systems. While some modal contributions will have little or no contribution in certain entries of **H**, some others will have major contributions. Therefore, the results presented in TABLE IX for different tolerances are for ULM only, and variable tolerance settings are adopted for modal contributions in FDCM.

The time domain simulation of Case-3 is shown in Fig. 7. As shown in Fig. 5, the cable sheaths are grounded by a 1 Ω resistance at both ends. The ac source is a Y-grounded source of 169 kV. The source impedance is characterized by its zero (0) and positive (1) sequence data in ohms ($R_0 = 2, R_1 = 1, X_0 = 22, X_1 = 1$). The switch closing times are: 0 s on phase-a, 0.63 ms on phase-b, and 0.4 ms on phase-c.

The results show that the waveforms for different models overlap. Zooming reveals small differences (below 0.01% relative error) between RKFIT and R-VFIT methods due to slightly different fitting outputs. The CPU performances in time domain show gains up to 15% with RKFIT.

TABLE IX CASE-3, FITTING RESULTS

ULM	**R-VFIT**		**RKFIT**	
Tolerance	1%	0.1%	1%	0.1%
Yc model order	11	20	20	20
Yc relative error	0.0092	0.0017	0.0074	0.0074
H model order	27	73	29	69
H max abs error	0.0089	8.4e-4	0.0074	6.01e-4
residue/pole ratio max	0.98	161	1.08	58
Passivity violation	No	Yes	No	Yes
FDCM	**R-VFIT**		**RKFIT**	
H model order	53		53	
H max abs error	0.0074		0.0074	
residue/pole ratio - max	0.70		0.57	

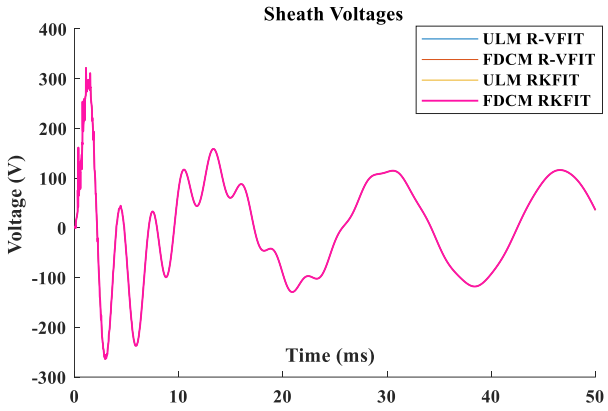

Fig. 7. Case-3, sheath voltages, R-VFIT, RKFIT for ULM and FDCM

4) Case-4: Underground Cable System, 9-phases

The cable system shown in Fig. 8 has 18 conductors. The cable parameters are presented in TABLE X . The fitting results are presented in TABLE XI.

In case of ULM, R-VFIT and RKFIT produce similar number of poles in the fitting of **H** and achieve the tolerance. R-VFIT cannot achieve the tolerance in the fitting of $\mathbf{Y_C}$ within the specified limit of order.

The models obtained with R-VFIT and RKFIT are used to perform a transient study, and it is observed that the simulation is unstable (see Fig. 9). The instability is explained with the combination of passivity violations and high residue-pole ratios with opposite signs that amplify integration and interpolation errors in time domain. As discussed before, increasing the number of conductors typically increases the likelihood of ULM producing larger residue-pole ratios that may result in unstable simulations.

An option is to switch to FDCM to resolve the instability. The fitting results show that, RKFIT and R-VFIT produce the same modeling order in FDCM. The models exhibit passivity violations at certain frequency samples, but these violations do not lead to instability as seen in Fig. 10. The passivity violation in RKFIT-FDCM is resolved when partitioned fitting in [8] is applied.

Transient analysis is performed using the FDCM. The phase-a of the first cable is energized with a step voltage of 1000 V. The sheaths are connected to each other and grounded at each end. The simulation time-step is $0.5\mu s$. The waveforms of the FDCM models produced by RKFIT and R-VFIT overlap.

As the overall fitting computation time will depend on several implementation factors due to the elaborate fitting procedures in FDCM and ULM, the performance test is conducted by computing the average computation times when different fitting algorithms are called per fixed number of poles in the fitting of $\mathbf{Y_C}$ in the phase domain. Calling the R-VFIT per iteration when the order is 20 in the fitting of $\mathbf{Y_C}$ takes 0.10 seconds whereas it takes 0.17 seconds for RKFIT. Fitting is an offline procedure performed only once or until a stable model is obtained. In other words, it is not necessary to perform fitting before each time domain simulation as long as the frequency dependent model is available. The fitting order, on the other hand, increases the simulation time in the time domain and it is an advantage to have models with less orders particularly in statistical studies or real time applications.

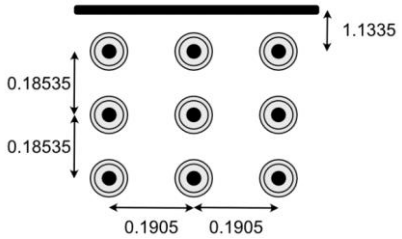

Fig. 8. Case-4, cable system, 9 cables

TABLE X CASE-4, CABLE PARAMETERS

Length	2 km
Inner radius of the core	0 mm
Outer radius of the core	12.38 mm
Inner radius of the sheath	24.69 mm
Outer radius of the sheath	25.33 mm
Outer insulation radius	27.34 mm
Resistivity of the sheath	1.7×10^{-8} Ohm m
Resistivity of the core	1.7×10^{-8} Ohm m
Core insulator relative permittivity	2.3
Shield insulator relative permittivity	2.48
Insulation loss factor	4×10^{-4}
Earth resistivity	100 Ohm m

TABLE XI CASE-4, FITTING RESULTS

ULM	**R-VFIT**	**RKFIT**
Tolerance	1%	1%
Yc model order	20	20
relative error	0.0129	0.0088
H model order	60	62
max abs error	0.0071	0.0046
Max residue/pole ratio	181300	3475
Passivity violation	Yes	Yes
FDCM	**R-VFIT**	**RKFIT**
H model order	162	162
H max abs error	0.0067	0.0067
H residue/pole ratio max	2.33	9.63
Passivity violation	Yes	Yes

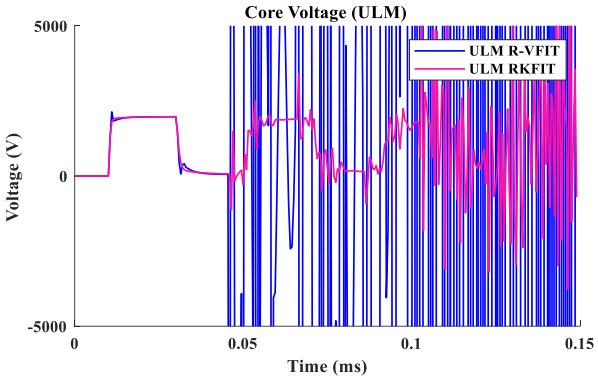

Fig. 9. Case-4, top core conductor voltage, R-VFIT and RKFIT with ULM

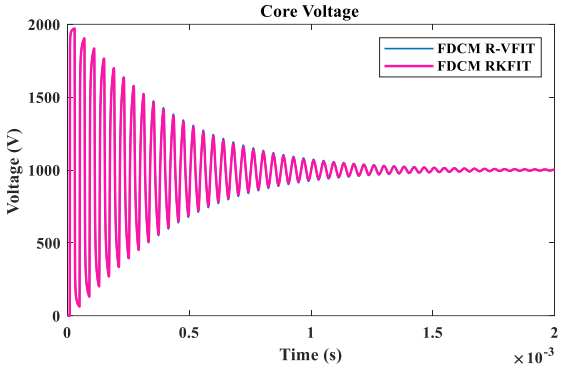

Fig. 10. Case-4, top left core end voltage, R-VFIT and RKFIT, FDCM

V. Conclusion

This paper presents stringent comparisons between VFIT, R-VFIT and RKFIT fitting techniques in the modeling of transmission lines and cables for electromagnetic transient simulations. Moreover, this paper contributes the application of RKFIT to the FDCM, which requires fitting modal contribution groups associated with a single delay term in the phase domain using a common set of poles. The resolution of an unstable ULM case with the application of the proposed fitting and modeling combination is also shown. It is also demonstrated that fitting of $\mathbf{Y}_C$ in the phase domain results in less error measured with 2-norm.

The presented test cases suggest that the proposed implementation with RKFIT delivers models with lower model orders compared to models obtained with the well-known VFIT technique. On the other hand, the RKFIT algorithm applied to ULM and FDCM presents marginal or no improvements over R-VFIT.

VI. References

[1] A. Morched, B. Gustavsen, and M. Tartibi, "A universal model for accurate calculation of electromagnetic transients on overhead lines and underground cables," *IEEE Trans. on Power Delivery*, 14(3):1032–1038, 1999.

[2] B. Gustavsen and A. Semlyen, "Rational approximation of frequency domain responses by vector fitting," *IEEE Trans. On Power Delivery*, Vol. 14, No. 3, pp. 1052–1061, Jul. 1999.

[3] B. Gustavsen, "Improving the pole relocating properties of vector fitting," in *IEEE Trans. On Power Delivery*, vol. 21, no. 3, pp. 1587-1592, Jul. 2006.

[4] B. Gustavsen, "Avoiding numerical instabilities in the universal line model by a two-segment interpolation scheme," *IEEE Trans. on Power Delivery*, vol. 28, No. 3, pp. 1643–1651, Jul. 2013.

[5] I. Kocar and J. Mahseredjian, "Accurate frequency dependent cable model for electromagnetic transients," *IEEE Trans. Power Delivery*, vol. 31, No. 3, pp. 1281–1288, Jun. 2016.

[6] F. Castellanos, J.R. Martí, F. Marcano, Phase domain multiphase transmission line models, International Journal of Electrical Power & Energy Systems, Volume 19, Issue 4, 1997, Pages 241-248.

[7] F. J. Marcano and J. R. Marti, "Idempotent line model: Case studies," Int. Conf. Power Syst. Transients IPST-1997, Seattle, WA, Jun. 1997.

[8] M. Cervantes, I. Kocar, J. Mahseredjian and A. Ramirez, "Partitioned Fitting and DC Correction for the Simulation of Electromagnetic Transients in Transmission Lines/Cables," *IEEE Trans. on Power Delivery*, 33(6):3246–3248, 2018.

[9] M. Berljafa. Rational Krylov Decompositions: Theory and Applications. PhD thesis, The University of Manchester, 2017.

[10] M. Berljafa and S. Güttel, "Generalized rational Krylov decompositions with an application to rational approximation. SIAM Journal on Matrix Analysis and Applications," 36 (2), 894-916, 2015.

[11] M. Berljafa and S. Güttel, A Rational Krylov Toolbox for MATLAB, MIMS, Manchester Institute for Mathematical Sciences, The University of Manchester, UK, 2014.

[12] M. Berljafa and S. Güttel, "The RKFIT Algorithm for Nonlinear Rational Approximation," Manchester Institute for Mathematical Sciences, The University of Manchester, Manchester, UK, 2015.

[13] A. Mouhaidali, D. Tromeur-Dervout, O. Chadebec, J-M. Guichon and S. Silvant, "Electromagnetic Transient Analysis of Transmission line based on rational Krylov approximation," *IEEE Trans. on Power Delivery*, vol. 36, no. 5, pp. 2913-2920, Oct. 2021.

[14] A. Ruhe. Rational Krylov: A practical algorithm for large sparse nonsymmetric matrix pencils, SIAM J. Sci. Comput., 19(5):1535--1551, 1998.

[15] A. Ruhe, Rational Krylov algorithms for nonsymmetric eigenvalue problems. II. Matrix pairs, Linear Algebra Appl., 198 (1994), pp. 283-295.

[16] A. Ruhe, The rational Krylov algorithm for nonlinear matrix eigenvalue problems, J. Math. Sci. (N. Y.), 114 (2003), pp. 1854-1856.

[17] A. Ruhe. The rational Krylov algorithm for nonsymmetric eigenvalue problems. III: Complex shifts for real matrices, BIT, 34:165--176, 1994.

[18] I. Kocar, J. Mahseredjian, and G. Olivier, "Improvement of numerical stability for the computation of transients in lines and cables," *IEEE Trans. on Power Delivery*, vol. 25, no. 2, pp. 1104–1111, Apr. 2010.

[19] A. Ramirez and R. Iravani, "Enhanced fitting to obtain an accurate dc response of transmission lines in the analysis of electromagnetic transients," *IEEE Trans. Power Del.*, vol. 29, No. 6, pp. 2614–2621, Dec. 2014.

[20] H. W. Bode, Network Analysis and Feedback Amplifier Design. Princeton, NJ: Van Nostrand, 1945.

[21] I. Kocar and J. Mahseredjian, "New Procedure for Computation of Time Delays in Propagation Function Fitting for Transient Modeling of Cables," *IEEE Trans. Power Del.*, vol. 31, no. 2, pp. 613-621, April 2016.

[22] B. Gustavsen, "Optimal Time Delay Extraction for Transmission Line Modeling," *IEEE Trans. Power Del.*, vol. 32, no. 1, pp. 45-54, Feb. 2017

[23] J. Mahseredjian, S. Dennetière, L. Dubé, B. Khodabakhchian and L. Gérin-Lajoie, "On a new approach for the simulation of transients in power systems," Electric Power Systems Research, vol. 77, no. 11, pp. 1514-1520, 2007.

[24] A. Haddadi, and J. Mahseredjian. "Power system test cases for *EMT-type* simulation studies." *CIGRE, Paris, France, Tech. Rep. CIGRE WG C* 4.2018 (2018): 1-142.